Corticospinal excitability is facilitated during coordinative action observation and motor imagery of adapted single-leg sit-to-stand movements in young healthy adults

Ashika Chembila Valappil[1], Neža Grilc[2], Federico Castelli[1], Samantha Chye[1], David J. Wright[3], Christopher J. Tyler[1], Ryan Knight[1], Omar S. Mian[1], Neale A. Tillin[1], Adam M. Bruton[1,2]

Author Note: Ashika Chembila Valappil is the first author for this manuscript. *Adam Bruton is the corresponding author for this manuscript: adam.bruton@brunel.ac.uk, HNZW 271, Heinz Wolff Building, Brunel University of London, Uxbridge, UB8 3PH, United Kingdom

School of Life and Health Sciences, University of Roehampton, United Kingdom
[2] Department of Sport, Health and Exercise Sciences, Brunel University of London, United Kingdom
[3] Department of Psychology, Manchester Metropolitan University, United Kingdom

Abstract

Combined action observation and motor imagery (AOMI) facilitates corticospinal excitability (CSE). This study used single-pulse transcranial magnetic stimulation (TMS) to explore changes in CSE for *coordinative* AOMI of a single-leg sit-to-stand (SL-STS) movement. Twenty-one healthy adults completed two testing sessions, where they engaged with baseline (BL), action observation (AO), and motor imagery (MI) control conditions, and three experimental conditions where they observed a *slow-paced* SL-STS while simultaneously imagining a *slow-* ($AOMI_{HICO}$), *medium-* ($AOMI_{MOCO}$), or *fast-paced* ($AOMI_{LOCO}$) SL-STS, with imagery guided through audio sonification. A TMS pulse was delivered to the right leg representation of the left primary motor cortex at three stimulation timepoints aligned with peak EMG activity of the knee extensor muscle group for the *slow-*, *medium-*, and *fast-paced* SL-STS during each condition. Motor evoked potential (MEP) amplitudes were recorded from the KE muscle group as a marker of CSE for all stimulation timepoints and conditions. A main effect for experimental condition was reported for all three stimulation timepoints. MEP amplitudes were significantly greater for $AOMI_{HICO}$ at T1 and T3, and $AOMI_{MOCO}$ and $AOMI_{LOCO}$ at all stimulation timepoints, when compared with control conditions. The findings provide empirical support for the propositions of the Dual-Action Simulation Hypothesis and Visual Guidance Hypothesis accounts for *coordinative* AOMI. This study builds on existing neurophysiological support for the use of *coordinative* AOMI as an alternative method for movement (re)learning. Longitudinal research incorporating neurophysiological and behavioral measures is warranted to explore the efficacy of *coordinative* AOMI for this purpose.

Keywords: Transcranial Magnetic Stimulation, Motor Evoked Potential, Dual-Action Simulation, Visual Guidance Hypothesis, Mental Simulation

Introduction

Action observation (AO) is the process of purposefully observing human movement via video or live demonstration (Eaves et al., 2022), while motor imagery (MI) involves the internal mental rehearsal of one's own movement execution (MacIntyre et al., 2013). Both AO and MI are effective interventions for enhancing movement execution and (re)learning in rehabilitation and care settings (e.g., Buccino, 2014; Herranz-Gómez et al., 2020; Nicholson et al., 2019). These improvements have been explained by motor simulation theory, which posits that AO and MI partially activate brain areas associated with movement planning, production, and control, and thus have the capacity to increase functional connectivity across these motor networks (Jeannerod, 2001). In support of this proposition, research employing a range of neuroscientific modalities (i.e., fMRI, fNIRS, EEG, TMS) demonstrates increased cortico-motor activity for both AO and MI compared to control/baseline conditions (see e.g., Condy et al., 2021; Grosprêtre et al., 2016; Hardwick et al., 2018). Literature to-date has typically compared these two forms of motor simulation, showing that brain activation patterns for AO and MI are distinct, but overlapping (Hardwick et al., 2018), and that both AO and MI facilitate corticospinal excitability (CSE) compared to control conditions (e.g., Clark et al., 2004; Williams et al., 2012). After an initial review by Vogt et al. (2013), a body of work has investigated the behavioral outcomes and underlying neurophysiological mechanisms associated with the combined use of AO and MI.

Combined action observation and motor imagery (AOMI) involves a person observing human movement and simultaneously imagining the physiological sensations and kinesthetic experiences associated with them executing the same or a different movement (Eaves, Riach, et al., 2016, Eaves et al., 2022). A recent meta-analysis by Chye and colleagues (2022) reported improved movement outcomes and increased facilitation of CSE for AOMI compared to AO and control, but not MI conditions. This meta-analysis synthesized literature on *highly-coordinated* AOMI ($AOMI_{HICO}$), where a person watches a movement demonstration and imagines the feeling of executing an identical

48 movement in the same perspective in time with the viewed content. The behavioral and
49 neurophysiological findings from Chye et al.'s (2022) meta-analysis suggest that $AOMI_{HICO}$ benefits motor
50 execution due to strong and widespread activation of movement-related brain regions. Specifically,
51 repeated engagement in $AOMI_{HICO}$ is likely to induce plastic-like changes in the motor system,
52 benefitting physical execution of the movement in a similar manner to physical training (Wright et al.,
53 2022). This sentiment is supported in a rehabilitation context, as studies employing TMS show that
54 $AOMI_{HICO}$ leads to increased facilitation of CSE for whole-body functional movements such as walking
55 (e.g., Kaneko et al., 2018) and balance (e.g., Mouthon et al., 2015, 2016), and studies employing
56 $AOMI_{HICO}$ as a training intervention report improved muscle strength (Scott et al., 2018), rehabilitation
57 outcomes (Marusic et al., 2018), and postural control (Taube et al., 2014) across the lifespan.
58 Whilst empirical support for $AOMI_{HICO}$ is growing, there is limited research on alternative forms
59 of AOMI. Vogt et al. (2013) introduced the idea that AOMI exists along a spectrum, whereby MI serves
60 different roles during AO depending on the level of coordination between the two. At one end of this
61 spectrum is *congruent* AOMI, where the content and/or visual perspective are identical for AO and MI
62 components of AOMI. The term $AOMI_{HICO}$ has been adopted instead of *congruent* AOMI in this study, as
63 it has been proposed that the AO and MI components are never fully *congruent* during AOMI (Frank et
64 al., 2020). This proposition was largely based on the different modalities adopted for AO (visual and
65 auditory) and MI (kinesthetic) components in Vogt et al.'s (2013) definition for *congruent* AOMI,
66 however it is worth noting that parameters such as body structure, movement pattern, and imagery
67 ability will also result in an offset between AO and MI during AOMI of the same action, making $AOMI_{HICO}$
68 a more suitable term. On the other end of the spectrum lies *conflicting* AOMI, where the content and/or
69 visual perspective for AO and MI components of AOMI are opposing (e.g., watching movement and
70 imagining being still and relaxed). In between these endpoints lies *coordinative* AOMI, where the
71 content and/or visual perspective for AO and MI components of AOMI is similar. For this type of AOMI,

72 the level of coordination between the observed or imagined actions can vary on a range of movement
73 parameters, including the type, direction, speed, force, and accuracy of the movement (Chye et al.,
74 2022; Grilc et al., 2024).

75 Two main theoretical hypotheses have been proposed to explain the underlying mechanisms for
76 *coordinative* AOMI. The first is the Dual-Action Simulation Hypothesis (DASH) account for AOMI
77 proposed by Eaves, Riach and colleagues (2016). Drawing from the Affordance-Competition Hypothesis
78 (Cisek, 2007), the DASH suggests that individuals generate separate motor representations for the
79 observed and imagined actions during AOMI, and that these are maintained as parallel sensorimotor
80 streams that either merge or compete depending on the level of coordination between the observed
81 and imagined actions. For $AOMI_{HICO}$ these likely merge as one sensorimotor stream, producing more
82 widespread activation in the premotor cortex compared to AO or MI alone. For lowly-coordinated AOMI
83 ($AOMI_{LOCO}$), where there is little overlap between the AO and MI components, the DASH proposes that
84 visuo-motor representations for the observed and imagined actions are likely to compete as separate
85 sensorimotor streams. This would result in similar cortico-motor activity to performing the AO or MI
86 tasks in isolation, depending on which simulation process is prioritized based on relevance to the
87 ongoing motor plan. For moderately-coordinated AOMI ($AOMI_{MOCO}$), the visuo-motor representations of
88 the observed and imagined movements may either merge or compete. This is dependent on the amount
89 of transferable sensorimotor information between the two simulated movements and the relevance of
90 these to the ongoing movement plan. Based on this proposition, $AOMI_{MOCO}$ can result in more
91 widespread pre-motor activity via merged sensorimotor streams, or similar activity to AO or MI alone
92 through prioritization of one competing sensorimotor stream, depending on the level of coordination
93 between the two simulated movements during this type of AOMI.

94 The Visual Guidance Hypothesis (VGH; Meers et al., 2020) has been proposed as an alternative
95 account for the processes involved in *coordinative* AOMI. The VGH argues that the imagined action is

96 prioritized, with the observed action serving as an external visual stimulus that may facilitate or disrupt
97 the imagined action during *coordinative* AOMI. According to the VGH, the increased cortico-motor
98 activity reported in previous literature for $AOMI_{HICO}$ (see Chye et al., 2022 for a recent meta-analysis) is
99 due to the observed action displaying *the same movement* and acting as a visual primer that forms a
100 stronger motor representation for the imagined action. For $AOMI_{LOCO}$, the VGH suggests that a motor
101 representation will only be formed for the imagined action due to the observed action displaying
102 *another movement* and acting as a visual distractor. Unless ignored, this will disrupt the generation and
103 maintenance of the imagined action, meaning cortico-motor activity will be reduced compared to
104 independent MI. In a similar vein to $AOMI_{LOCO}$, the VGH proposes that a motor representation will only
105 be formed for the imagined action during $AOMI_{MOCO}$ due to the observed action displaying *another*
106 *movement*. However, the observed action might act as a visual primer or visual distractor during
107 $AOMI_{MOCO}$ depending on the amount of transferable sensorimotor information between the two
108 simulated movements. It is therefore possible that the observed action can both facilitate and disrupt
109 the generation and maintenance of the imagined action, leading to either increased, similar, or
110 decreased cortico-motor activity compared to independent MI.
111 Single-pulse TMS is the most prevalent neuroscientific modality adopted in the AOMI literature
112 as it has high temporal resolution and can be used to determine the specific contributions for observed
113 and imagined actions during AOMI (Chye et al., 2022). However, only three studies have used TMS to
114 examine the neurophysiological markers for *coordinative* AOMI, reporting somewhat conflicting findings
115 (Bruton et al., 2020; Meers et al., 2020; Grilc et al., 2024). Bruton et al. (2020) used a *coordinative* AOMI
116 task where participants observed an index finger abduction-adduction movement while imagining the
117 same movement with their little finger. They found that CSE was facilitated in the muscles controlling
118 both the observed and imagined movements, when controlling for visual attention on the observed
119 movement. Conversely, using a similar finger movement task, Meers et al. (2020) found that CSE was

only facilitated for the imagined finger movement, with no such facilitation for the observed finger movement during *coordinative* AOMI. In a recent TMS study, Grilc et al. (2024) utilized two different *coordinative* AOMI tasks where coordination between the observed and imagined actions was based on different movement parameters. Both *coordinative* AOMI tasks involved observation of a knee extension movement, with one task involving imagined plantarflexion of the foot, a movement that is typically coupled with a knee extension movement when the body is propelled forward or upward by the legs (i.e., coordinated based on functional coupling), and one task involving imagined dorsiflexion of the foot, a movement that rotates the foot in the same direction as the shank segment of the lower leg during knee extension, when both movements are viewed from the transverse plane (i.e., coordinated based on movement direction). CSE was facilitated in the muscle controlling the imagined foot movement for both *coordinative* AOMI conditions, regardless of movement parameter, but no such facilitation was identified for the observed lower-leg movement, aligning with the finding of Meers et al. (2020). The findings of Bruton et al. (2020) align with specific predictions of the DASH, whereas the findings of Meers et al. (2020) and Grilc et al. (2024) support the predictions of the VGH, suggesting both hypotheses warrant further empirical investigation by examining the neurophysiological markers of *coordinative* AOMI.

The limited research on *coordinative* AOMI may be due, in part, to the challenge of clearly defining the parameters that govern coordination between the two simulated actions. Both Bruton et al. (2020) and Meers et al. (2020) coordinated the observed and imagined actions based on movement type (finger abduction-adduction), whereas Grilc et al. (2024) employed two AOMI conditions that coordinated the observed and imagined actions based on different movement parameters (i.e., functional coupling vs movement direction). It is important to draw from literature on AO or MI when considering possible movement parameters that might influence the ability to coordinate observed and imagined actions, and the subsequent neurophysiological markers for *coordinative* AOMI. Several

144 studies have explored neurophysiological markers for AO and MI tasks with different force
145 requirements, showing that CSE is increased as a function of force production during both observed
146 (e.g., Alaerts et al., 2010, 2012; Helm et al., 2015) and imagined actions (e.g., Helm et al., 2015;
147 Mizuguchi et al., 2013). There are mixed findings regarding movement speed during AO, with studies
148 reporting decreased CSE (Moriuchi et al., 2014, 2017), no change in CSE (Moriuchi et al., 2017), and
149 increased CSE (Kitamura et al., 2023) as movement speed is increased for various upper-limb
150 movements. Given the close relationship between movement force and speed for dynamic actions,
151 where greater force often results in faster movement, manipulating one of these parameters is of
152 potential interest during *coordinative* AOMI.

153 This study aimed to test the DASH (Eaves, Riach, et al., 2016) and VGH (Meers et al., 2020)
154 propositions for *coordinative* AOMI by comparing CSE responses during AOMI conditions where
155 coordination between the observed and imagined actions varied based on movement speed. In this
156 experiment, all *coordinative* AOMI conditions involved observation of a *slow-paced* single-leg sit-to-
157 stand (SL-STS) movement but varied in the speed of the simultaneously imagined SL-STS. Specifically,
158 $AOMI_{HICO}$ involved simultaneous imagery of a *slow-paced* SL-STS, $AOMI_{MOCO}$ involved simultaneous
159 imagery of a *medium-paced* SL-STS, and $AOMI_{LOCO}$ involved simultaneous imagery of a *fast-paced* SL-STS
160 during observation of a *slow-paced* SL-STS.

161 If the propositions of the DASH (Eaves, Riach, et al., 2016) are accurate, it is hypothesized that:
162 H1; CSE facilitation will be increased for the $AOMI_{HICO}$ condition at T3 (i.e., the stimulation timepoint
163 corresponding to peak EMG activity for the *slow-paced* SL-STS) due to the merger of sensorimotor
164 streams for AO and MI of the same action and movement speed. H2; CSE facilitation will be increased
165 for the $AOMI_{MOCO}$ condition at both T3 and T2 (i.e., the stimulation timepoint corresponding to peak
166 EMG activity for the *medium-paced* SL-STS) due to the maintenance of sensorimotor streams for AO and
167 MI of the same action with similar movement speeds. H3; CSE facilitation will not be increased for the

168 $AOMI_{LOCO}$ condition at any stimulation timepoint due to the competition between sensorimotor streams
169 for AO and MI of the same action with different movement speeds.

170 If the propositions of the VGH (Meers et al., 2020) are accurate, it is hypothesized that: H1; CSE
171 facilitation will be increased for the $AOMI_{HICO}$ condition at T3 because the observed action will enhance
172 the motor representation formed for the imagined action when the same movement type and speed are
173 employed for both AO and MI simultaneously. H2; CSE facilitation will be increased for the $AOMI_{MOCO}$
174 condition at T2 due to prioritization of the imagined action during simultaneous AO and MI of the same
175 action with similar movement speeds. H3; CSE facilitation will be increased for the $AOMI_{LOCO}$ condition at
176 T1 due to prioritization of the imagined action during simultaneous AO and MI of the same action with
177 different movement speeds.

178 **Methods**

179 **Participants**

180 Based on previous AOMI studies employing TMS (e.g., Bruton et al., 2020; Grilc et al., 2024;
181 Wright et al., 2018), twenty-one healthy adults aged 21-43 years (66.7% male, M_{age} = 29.29 ± 6.78 years)
182 with normal or corrected-to-normal vision took part in this study. All participants underwent screening
183 and provided written informed consent prior to data collection. The screening included completion of
184 the TMS Adult Safety Screen (TASS; Keel et al., 2001) and the Movement Imagery Questionnaire - 3
185 (MIQ-3; Roberts et al., 2008). All participants were safe to take part in the study based on responses to
186 the TASS. MIQ-3 scores indicated that the final study sample could easily generate internal visual (6.14 ±
187 0.66), external visual (5.71 ± 1.27), and kinesthetic (5.57 ± 1.22) imagery, confirming their ability to
188 complete the experimental tasks.

189 **Experimental Design**

190 This study was conducted in accordance with the ethical guidelines and approval of the
191 University of Roehampton ethical committee. All study procedures are reported using parts A, B and C

192 of the Guidelines for Reporting Action Simulation Studies checklist (Moreno-Verdú et al., 2024) and
193 experimental code and materials can be accessed via the Open Science Framework:
194 https://osf.io/5vjwe/. A repeated measures design was employed where participants completed six
195 conditions, split into three control conditions and three experimental conditions. The three control
196 conditions included: (i) a baseline (BL) condition where participants looked at a fixation cross placed on
197 an image depicting the SL-STS from the video stimuli (50% of trials) or a blank background (50% of
198 trials), (ii) an action observation (AO) condition where participants were required to observe a video of a
199 model performing a *slow-paced* SL-STS movement, and (iii) a motor imagery (MI) condition where
200 participants were required to imagine the feelings and sensations associated with performing a *slow-*
201 *paced* SL-STS movement. The three experimental conditions included: (iv) a highly-coordinated AOMI
202 ($AOMI_{HICO}$) condition where participants were asked to simultaneously observe a *slow-paced* SL-STS
203 movement while imagining the feelings and sensations of performing the same *slow-paced* SL-STS
204 movement, (v) a moderately-coordinated AOMI ($AOMI_{MOCO}$) condition where participants were asked to
205 simultaneously observe a *slow-paced* SL- STS movement while imagining the feelings and sensations of
206 performing a *medium-paced* SL-STS movement, and (vi) a lowly-coordinated AOMI ($AOMI_{LOCO}$) condition
207 where participants were asked to simultaneously observe a *slow-paced* SL-STS movement while
208 imagining the feelings and sensations of performing a *fast-paced* SL-STS movement.
209 The six conditions were presented in a semi-randomized order across participants (see Figure 1
210 for a visual depiction of the experimental design), to coincide with previous TMS studies investigating
211 different forms of AOMI (e.g., Bruton et al., 2020; Grilc et al., 2024). The BL condition was delivered
212 across five blocks of six trials (i.e., blocks 1, 3, 5, 7, 9) to account for a possible ordering effect across the
213 experiment by recording comparator MEP amplitude data before each condition containing movement
214 simulation tasks. The AO condition was presented as block 2, before any MI instructions were provided,
215 to reduce the likelihood of participants engaging in spontaneous or deliberate MI during this condition.

The MI condition was presented as block 4, after AO, as it was deemed necessary to have first exposed participants to visual stimuli of a SL-STS to facilitate their MI of the action due to their naivety with this movement. The three experimental conditions involving *coordinative* AOMI tasks were presented last (i.e., blocks 6, 8, and 10), with the order of these counterbalanced across the study sample to avoid the possibility of an ordering effect for these conditions.

Target Movement

The SL-STS, a gross motor task that requires strength, balance, and coordination, was chosen as the target movement in this study. This movement was selected because the ability to safely rise from sitting to standing is fundamental to many activities of daily living (Slaughter et al., 2015), and approximately 25% of falls occur when an older person is either rising from or lowering on to a chair (Robinovitch et al., 2013). Young healthy adult performance of the SL-STS is representative of bipedal sit-to-stand execution in older adults as both tasks rely on sufficient lower-limb strength (Tapanya & Chamnongkich, 2014), with relative muscle power declining above the age of 40 years old (Alcazar et al., 2020). Use of this target movement make the findings of this study applicable to older adult populations in the context of falls. The SL-STS task began with participants seated on a height-adjustable stool, with their left leg hovering off the floor and the right foot planted firmly on the ground, maintaining a 90-degree flexion of the knee. Participants were instructed to sit on the edge of the seat, their arms across their chest, resting their hands on opposite shoulders. To execute the SL-STS movement, participants pushed through the heel of the planted foot, engaging the leg and core muscles to rise to a standing position while maintaining balance. The task was performed at three different speeds (*slow-*, *medium-*, and *fast-paced*) for five repetitions during the familiarization phase of the study. To help participants time their movements, sonification cues were provided.

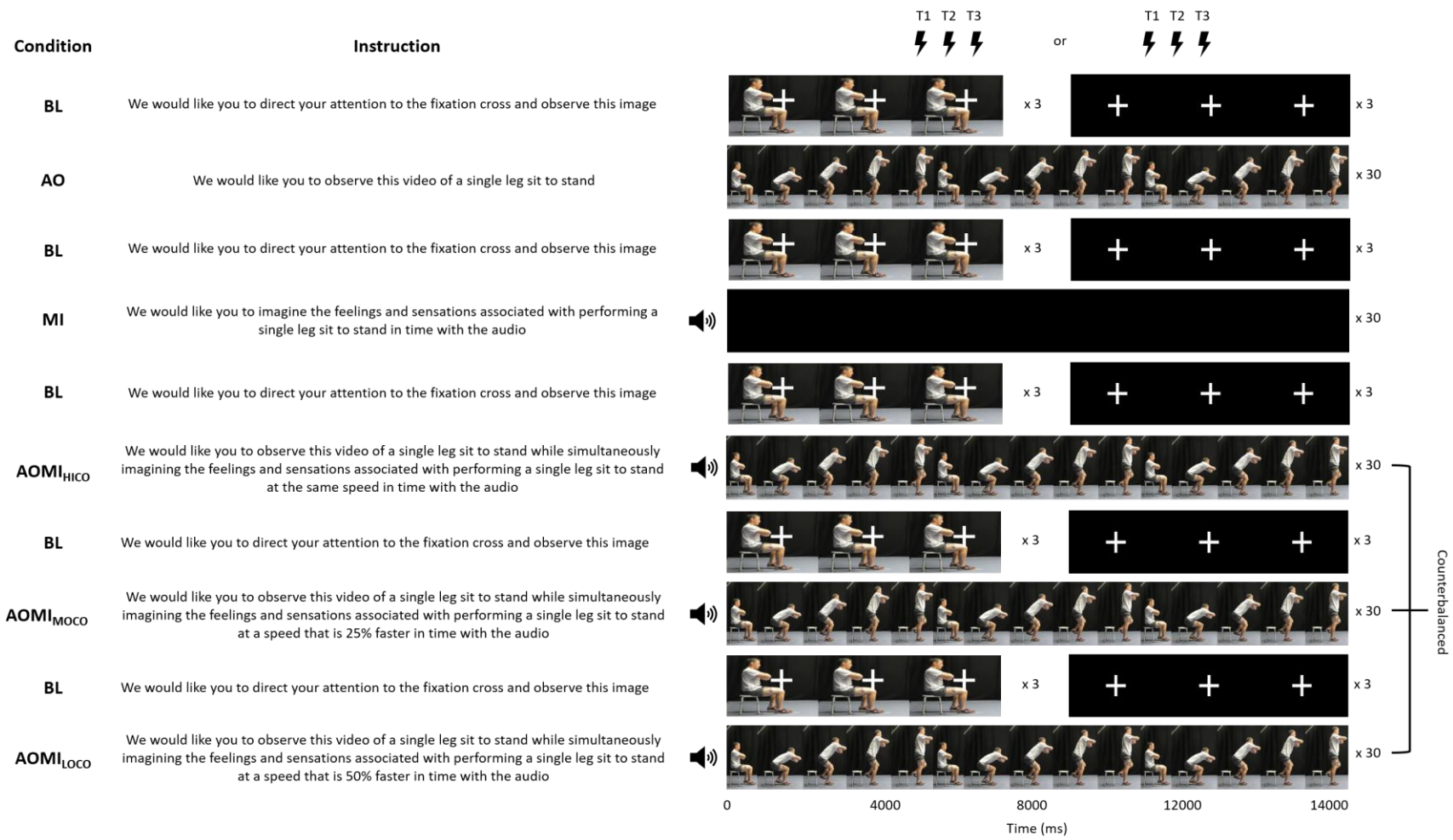

Figure 1. A Visual Representation of the Ten Experimental Blocks Completed During Each Testing Session. *Note:* The TMS was delivered at the point of peak EMG activity in the knee extensor muscle group for the models performing the *fast-paced* (T1), *medium-paced* (T2), and *slow-paced* (T3) SL-STS for either the second or third cycle of every AOMI trial, and at the same time point for trials in control conditions. The ordering of the TMS delivery was randomized and counterbalanced across trials for each experimental block. The model depicted in figure 1 is an author of the study.

244 **Stimuli Development**

245 Timings for the *slow-, medium-* and *fast-paced* SL-STS movements depicted in the video and
246 audio stimuli used in this study were determined through pilot testing given the novelty of the selected
247 target movement. Five pilot participants (4 male, 1 female) completed five successful trials of the SL-STS
248 under instructions to move (i) as slowly as possible (i.e., *slow-paced*), (ii) at a 'normal' pace (i.e.,
249 *medium-paced*), and (iii) as quickly as possible (i.e., *fast-paced*). During these trials, pilot participants
250 were fitted with a reflexive marker on the C7 vertebra to identify movement start and end points using a
251 12-camera Vicon Vantage motion capture system (Vicon, Oxford, UK) sampling at 100Hz. Surface
252 electromyography (EMG) activity was recorded for the vastus lateralis (VL), vastus medialis (VM) and
253 rectus femoris (RF) muscles using a single bipolar silver-chloride gel-electrode configuration (2-cm
254 diameter, 2-cm inter-electrode distance; Dual Electrode, Noraxon, Arizona, U.S.A.) to detect the point of
255 peak EMG activity for the *slow-*, *medium-* and *fast-paced* SL-STS movements. On average across the pilot
256 participants, the *slow-paced* SL-STS trial lasted 3.76 ± 1.23 seconds, the *medium-paced* SL-STS trial lasted
257 2.34 ± 0.38 seconds, and the *fast-paced* SL-STS trial lasted 1.69 ± 0.29 seconds. The average *medium-*
258 *paced* SL-STS trial was closer in timing to the *fast-paced* SL-STS trial, meaning the midpoint between the
259 *slow-* and *fast-paced* SL-STS (i.e., 2.73 seconds) was selected as the timing for the *medium-paced* SL-STS.

260 One male and one female model were selected for development of the video stimuli. The
261 models were video recorded performing the *slow-paced* SL-STS movement in the sagittal plane (see
262 Figure 2) using a Panasonic camera (HC-W570, 1920x1080 resolution and 50 frames per second). A
263 metronome was used so that both models could match the selected timings for the *slow-, medium-*, and
264 *fast-paced* SL-STS as closely as possible. The research team agreed upon the model's best trial for the
265 different SL-STS speeds by considering the time-discrepancy between the target and executed trial
266 durations, and the perceived smoothness of the executed SL-STS movement. Peak EMG activity in the
267 VM, VL, and RF was identified for the selected SL-STS trials using a bespoke Matlab (R2020a The

MathWorks) script. The time at peak EMG activity was averaged across the knee extensor (KE) muscles for the best trial of each model and used to determine TMS stimulation timepoints for the different conditions (see Figure 3 for EMG profiles). The total SL-STS trial times were used to produce movement sonification files on the open-source software Audacity (Audacity Team version 2.4.1) to guide MI timing during conditions where this was required (i.e., the MI control condition and three experimental conditions).

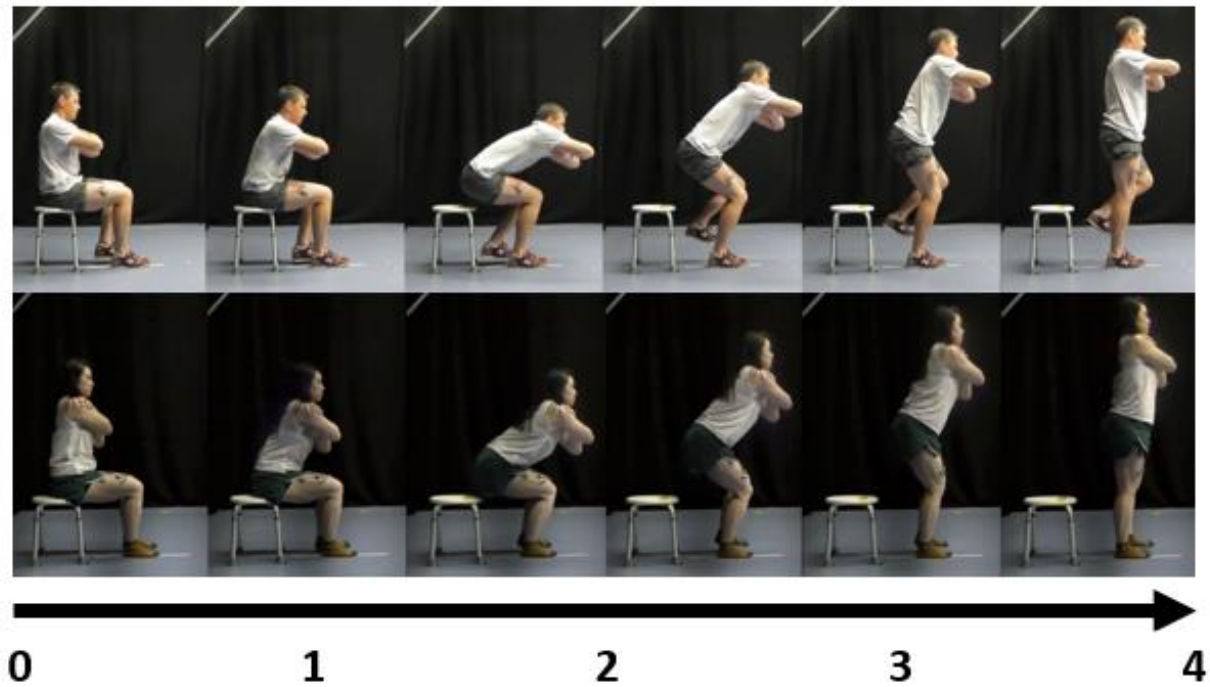

Figure 2. A visual depiction of the male (top) and female (bottom) models performing the *slow-paced* SL-STS used as the video stimuli in the AO control condition and AOMI experimental conditions used in this study. *Note:* The timing differed across the models, with the male model taking 3740ms and the female model taking 3660ms to complete the *slow-paced* SL-STS used in the video stimuli. Both the models depicted in figure 2 are authors of the study.

Experimental Procedure

Surface Electromyography Preparation and Recording

Prior to EMG placement, the skin was prepared by shaving and cleaning the area where EMG electrodes were placed. The EMG system adopted for stimuli development was used to measure EMG

activity for the three KE muscles of the participants' right leg during the main experimental protocol. The EMG sensors (DTS-EMG sensors, Noraxon, USA) and electrodes were attached to the muscle belly of the target muscles based on the SENIAM (Hermens et al., 1999) guidelines. Noraxon wireless sensors (bandwidth of 20–450 kHz, 92 dB common mode rejection ratio and > 1015 Ω input impedance) transmitted the EMG signals to a desktop receiver (TeleMYO DTS EMG; Noraxon, Arizona, USA), and these were sampled at 2 kHz via an analogue-to-digital convertor (Micro 1401–3) and desktop PC utilizing Spike2 software (Cambridge Electronic Design, Cambridge, UK).

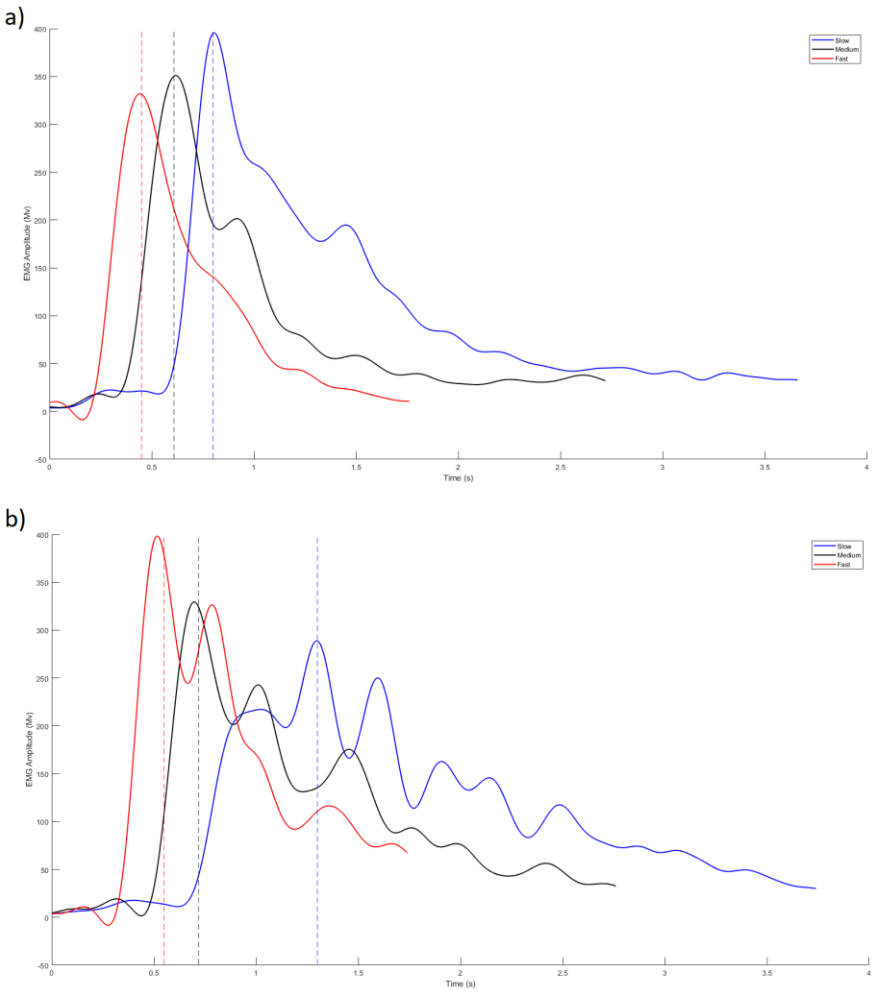

Figure 3. Figures displaying EMG traces for the (a) female and (b) male models performing the *slow-paced* (blue), *medium-paced* (black), and *fast-paced* (red) SL-STS during pilot data collection that was used to determine the TMS stimulation timepoints corresponding with the different SL-STS speeds. *Note:* The three TMS stimulation timepoints are denoted on the figure by color-matched vertical dashed lines.

297 ***Transcranial Magnetic Stimulation Preparation***

298 **Optimal Scalp Position.** The TMS preparation procedures adhered to methodological guidelines,
299 as recorded via a methodological reporting checklist for TMS experiments (Chipchase et al., 2012).
300 Participants were fitted with a tight-fitting polyester cap with the center of the scalp (i.e., Cz), defined by
301 the intersection of lines from inion to nasion and from left to right tragus, measured and marked as the
302 top-right most corner of a 3x3cm grid drawn for identification of the optimal scalp position (OSP). A
303 single-pulse double-cone coil TMS (110 mm diameter) connected to a Magstim 200^2 monophasic
304 magnetic stimulator was originally placed at Cz and oriented to direct current flow from anterior to
305 posterior. The TMS coil was manually moved around the 3x3cm grid in 0.5cm intervals posterior and
306 lateral from Cz, and four stimulations were delivered at each site to identify the OSP that produced the
307 largest and most consistent MEP amplitudes across the three KE muscles. OSP sites ranged from 0.5-
308 2.5cm posterior and 0-1.5cm lateral to Cz, with the median OSP coordinates recorded as 1cm posterior
309 and 0.5cm lateral across the study sample.

310 **Resting Motor Threshold.** The resting motor threshold (RMT; excitability of the KE muscle
311 representation of the motor cortex at rest) was determined following the guidelines of Rossini et al.
312 (2015). This involved gradually reducing the stimulation intensity in 5% increments from the
313 participants' OSP intensity until five out of ten trials produced MEP amplitudes exceeding 50 µV in at
314 least two out of three KE muscles. Consistent with previous TMS literature on AOMI, the experimental
315 stimulation intensity was set at 110% of the RMT (Bruton et al., 2020; Wright et al., 2018) to minimize
316 direct wave stimulation (Loporto et al., 2013). The mean RMT was 64 ± 11% and the mean experimental
317 stimulation intensity was 71 ± 12% of the maximum stimulator output, both similar values to that of a
318 recent TMS experiment investigating AOMI in lower-leg muscles (see Grilc et al., 2024).

Experimental Setup

The participants were seated comfortably on a Norm isokinetic dynamometer chair (Cybex Norm Testing & Rehabilitation System, Cybex Norm Inc., Ronkonkoma, USA) in a dimly lit Biomechanics Laboratory at the host university, with their upper body loosely strapped in place to reduce movement or repositions during the experimental block and maintain a consistent viewing position between blocks. The video stimuli were presented on an 80" adjustable screen (LED Interactive Multi-Touch Display, model 86GT-4K, SHENZHEN Hitevision Technology Co., Ltd.) placed 130cm directly in front of the participant using DMASTR DMDX display software (Forster & Forster, 2003).

Familiarization

A familiarization phase was incorporated for all conditions where MI was instructed (i.e., MI, $AOMI_{HICO}$, $AOMI_{MOCO}$, $AOMI_{LOCO}$) to guide the participants' engagement with the upcoming observed and imagined movements. During this phase, participants watched five repetitions of a model performing the SL-STS at the required speed whilst seated on an adjustable stool with arms placed diagonally across their chest. After this, the participants physically practiced the movement for five repetitions, matching their speed to the speed of the model in the demonstration video. A further five physical repetitions were then completed, with the addition of the audio sonification file overlaid onto the video of the model performing the SL-STS at the speed to be imagined. The final step involved the participants receiving instructions to engage with MI of the SL-STS in time with the audio sonification of the movement whilst being presented with a video of a *slow-paced* SL-STS for the experimental conditions, or image of a blank screen for the MI condition.

Experimental Protocol

The experimental protocol was repeated across two 3-hour testing sessions, at least 48 hours apart. In each testing session, the participants completed ten experimental blocks consecutively, with the five BL blocks lasting 90sec and the five main experimental blocks (i.e., AO, MI, $AOMI_{HICO}$, $AOMI_{MOCO}$,

343 $AOMI_{LOCO}$) lasting 450sec per block. A 180sec rest period was included after each of the main
344 experimental blocks, and participants were encouraged to leave the testing chair to prevent eye strain
345 and muscular discomfort before familiarizing themselves with the stimuli and task for the next
346 experimental block. Prior to beginning the experiment, participants were asked to read the on-screen
347 instructions carefully, refrain from voluntary movement during the experimental blocks, and to attend
348 fully to the stimuli presented. Understanding of these instructions was verbally confirmed before the
349 start of each block. The 30-trial main experimental block incorporated a rest period after each set of 10
350 trials. Written and verbal reminders of the specific instructions for the condition were provided before
351 the participant completed each set of 10 trials. All trials were displayed on the LCD screen using
352 DMASTR DMDX display software (Forster & Forster, 2003) and lasted 10980ms for female participants
353 and 11220ms for male participants. For the AO control condition and three AOMI experimental
354 conditions (see Figures 1 and 2 for stimuli and instructions), the trials showed three repetitions of a
355 *slow-paced* SL-STS (3660ms per cycle for females, 3740ms per cycle for males). When observing the
356 *slow-paced* SL-STS, participants were instructed to simultaneously imagine the feelings and sensations
357 associated with a slow- ($AOMI_{HICO}$), *medium*- ($AOMI_{MOCO}$), or *fast-paced* SL-STS ($AOMI_{LOCO}$) using audio
358 sonification files lasting 100%, 75% and 50% of the *slow-paced* SL-STS duration for respective guidance.
359 For the MI condition, the participants observed a blank screen and engaged with MI following the same
360 instructions and audio sonification as the $AOMI_{HICO}$ condition.

361 ***TMS Data Collection***

362 Using a script run through Spike 2 software, a single TMS pulse was delivered once per trial
363 during the second (female = 3661-7320ms, male = 3741-7580ms) or third (female = 7321-10980ms,
364 male = 7581-11220ms) cycles of the observed *slow-paced* SL-STS movement used in the three
365 experimental and AO conditions, and at the corresponding time points for the trials for the BL and MI
366 control conditions. Participants were stimulated during two cycles of the SL-STS movement to reduce

367 the predictability of the stimulation and subsequent anticipatory behavior of the participants (Loporto
368 et al., 2012). TMS stimulation timepoints represented the point of peak EMG activity for the two models
369 when physically performing the different paced SL-STS trials used to produce the video and audio stimuli
370 for this study. TMS stimulation timepoints corresponding to the *fast*- (T1; female = 450ms, male = 550ms
371 after cycle onset), *medium*- (T2; female = 610ms, male = 720ms after cycle onset) and *slow-paced* SL-STS
372 (T3; female = 800ms, male = 1300ms after cycle onset) were randomly ordered and counterbalanced
373 within-conditions. A 3sec transition period was implemented between experimental trials to maintain
374 an inter-stimulus interval greater than 10 seconds to let the effects of the preceding TMS pulse diminish
375 (Chen et al., 1997).

376 ***Social Validation Data Collection***

377 Ratings of perceived MI ability were recorded using a 7-point Likert scale from 1 (very easy to
378 feel) to 7 (very hard to feel) at the end of the familiarization phase, during the break periods between
379 each block of 10 trials, and at the end of the experiment for the conditions involving engagement with
380 MI processes (i.e., MI, $AOMI_{HICO}$, $AOMI_{MOCO}$, $AOMI_{LOCO}$). After finishing the TMS data collection for the
381 second testing session, participants recorded social validation data in a similar fashion to recent AOMI
382 experiments using TMS (e.g., Bruton et al., 2020; Grilc et al., 2024; Riach et al., 2018). Initially,
383 participants recorded responses on a bespoke social validation questionnaire, where they rated
384 perceived sex and ownership of the modeled SL-STS movements displayed in the conditions with an AO
385 component (i.e., AO, $AOMI_{HICO}$, $AOMI_{MOCO}$, $AOMI_{LOCO}$) using three 5-point Likert scales from 1 (totally
386 disagree) to 5 (totally agree). Participants then took part in a semi-structured social validation interview
387 designed to understand their experiences across the different conditions and check for compliance with
388 the intended manipulations.

389 **Data Analysis**

390 ***TMS Data Processing***

391 Peak-to-peak MEP amplitudes were recorded from the three KE muscles (VM, VL and RF) of the
392 participants' right leg on a trial-by-trial basis and averaged across all successful trials for T1, T2 and T3
393 TMS stimulation timepoints per condition. After extracting the data from Spike 2, and separating the
394 data based on TMS stimulation timepoint, a two-part screening process was used to determine
395 successful trials. First, trials were screened for the presence of an MEP response, and any trials that did
396 not evoke an MEP amplitude of sufficient magnitude (i.e., 50 µV) were removed. It is reported that MEP
397 amplitudes are increased for a target muscle if the EMG activity in that muscle is above resting state
398 levels at, or immediately prior to, the time of TMS stimulation (Devanne et al., 1997; Hess et al., 1987).
399 To control for this, EMG activity was recorded for 200 ms prior to the delivery of each TMS pulse and
400 any trials where the EMG amplitude exceeded normal baseline values (mean ± 2.5 SD) for that TMS
401 stimulation timepoint and condition were removed (e.g., Riach et al., 2018; Wright et al., 2014; 2018).
402 For the study sample, a mean value of 4.71 (± 3.93) trials for the VM muscle, 6.66 (± 6.05) trials for the
403 VL muscle, and 2.35 (± 2.59) trials for the RF muscle were removed per TMS stimulation timepoint and
404 condition. This resulted in the sample having a mean value of 19.22 (± 4.69) trials with an
405 uncontaminated MEP response in one or more KE muscles, providing a reliable estimate of CSE per TMS
406 stimulation timepoint and condition (Cuypers et al., 2014). On a muscle-by-muscle basis, the raw MEP
407 amplitude data for successful trials was normalized using a *z*-score transformation to account for the
408 large intra- and inter-participant variability in MEP amplitudes at rest (e.g., Bruton et al., 2020; Grilc et
409 al., 2024; Wright et al., 2014). For each participant, this procedure involved standardizing the MEP
410 amplitude value recorded for each successful trial against all other MEP amplitude values recorded for
411 successful trials for that TMS stimulation timepoint across the two testing sessions. The mean amplitude
412 for all successful trials at each TMS stimulation timepoint (i.e., T1, T2, T3) was represented by a value of

zero, and values for each condition were denoted by how many standard deviations that condition was above or below the mean of all conditions. Once the *z*-score transformation was complete, the mean *z*-score MEP amplitude value was recorded for the three KE muscles on a trial-by-trial basis. This mean was calculated from three KE muscles for 70.41%, two KE muscles for 19.83%, and one KE muscle for 9.76% of successful trials. For all participants, a mean *z*-score MEP amplitude value was calculated per condition at each TMS stimulation timepoint for analysis.

TMS Data Analysis

The *z*-score MEP amplitude data for the KE muscles was normally distributed at each TMS stimulation timepoint, permitting the use of analysis of variance (ANOVA) statistical tests. Three separate one-way repeated measure ANOVA tests with six levels (Condition: BL, AO, MI; $AOMI_{HICO}$; $AOMI_{MOCO}$; $AOMI_{LOCO}$) were run using the rstatix package (Kassambara, 2023) and the data was visualized using the ggplot2 package (Wickham, 2016) in R studio statistical software (version 4.3.2). Bonferroni contrasts were used for post-hoc pairwise comparisons. Outlier analysis was conducted using interquartile range values, and data points identified as outliers were removed from the three ANOVA analyses (T1 = 2, T2 = 2, T3 = 3 outliers). To test for a potential ordering effect across the experiment, a one-way repeated measure ANOVA test with five levels (BL block: block 1, block 3, block 5, block 7, block 9) was conducted for *z*-score MEP amplitude data recorded in BL experimental blocks. For this comparison, the *z*-score transformation was conducted based on the data from the 60 BL trials collected across the two testing sessions. A one-way repeated measures ANOVA analysis performed on the BL condition *z*-score MEP amplitude data revealed no significant main effect of block, $F_{(4, 72)} = 1.01$, $p = .41$, $\eta_p^2 = .05$.

Social Validation Data Analysis

A one-way repeated measures ANOVA with four levels (Condition: MI; $AOMI_{HICO}$; $AOMI_{MOCO}$; $AOMI_{LOCO}$) was run on the perceived MI ability data collected from the social validation questionnaire to

investigate differences across the conditions with MI processes. An independent samples t-test (Participant Sex: male; female) was run on the perceived body ownership, masculinity, and femininity data collected from the social validation questionnaire to investigate differences in male and female participants' ratings of the movements displayed across the conditions with AO processes. Interview data was transcribed, coded, and grouped on a question-by-question basis to offer detailed explanations for the MI ability ratings from the social validation questionnaire.

Results

MEP Amplitude Data

One-way repeated measures ANOVA analyses performed on the *Z*-score MEP amplitude data revealed a significant large main effect of condition at T1, $F_{(5, 90)} = 8.28$, $p < .001$, $\eta_p^2 = .31$, T2, $F_{(3.04, 54.69)} = 8.32$, $p < .001$, $\eta_p^2 = .31$, and T3, $F_{(5, 85)} = 18.4$, $p < .001$, $\eta_p^2 = .51$, TMS stimulation timepoints. Post-hoc pairwise comparisons between the experimental conditions (i.e., $AOMI_{HICO}$, $AOMI_{MOCO}$, $AOMI_{LOCO}$) and control conditions (i.e., BL, AO, MI) across the three TMS stimulation timepoints are reported below.

Highly-Coordinated AOMI ($AOMI_{HICO}$)

Post-hoc pairwise comparisons at T3 (Figure 3), the TMS stimulation timepoint corresponding to the *slow-paced* SL-STS, showed that *Z*-score MEP amplitudes were significantly larger in the $AOMI_{HICO}$ condition compared to the BL ($p < .001$) and AO ($p < .001$) conditions, but not the MI condition ($p = .29$). Post-hoc pairwise comparisons at T2 (Figure 4), the TMS stimulation timepoint corresponding to the *medium-paced* SL-STS, showed no significant differences between the $AOMI_{HICO}$ condition and the three control conditions (*p*s > .05). Post-hoc pairwise comparisons at T1 (Figure 5), the TMS stimulation timepoint corresponding to the *fast-paced* SL-STS, showed that *Z*-score MEP amplitudes were significantly larger in the $AOMI_{HICO}$ condition compared to the BL ($p = .01$) and AO ($p < .001$) conditions, but not the MI condition ($p = .34$).

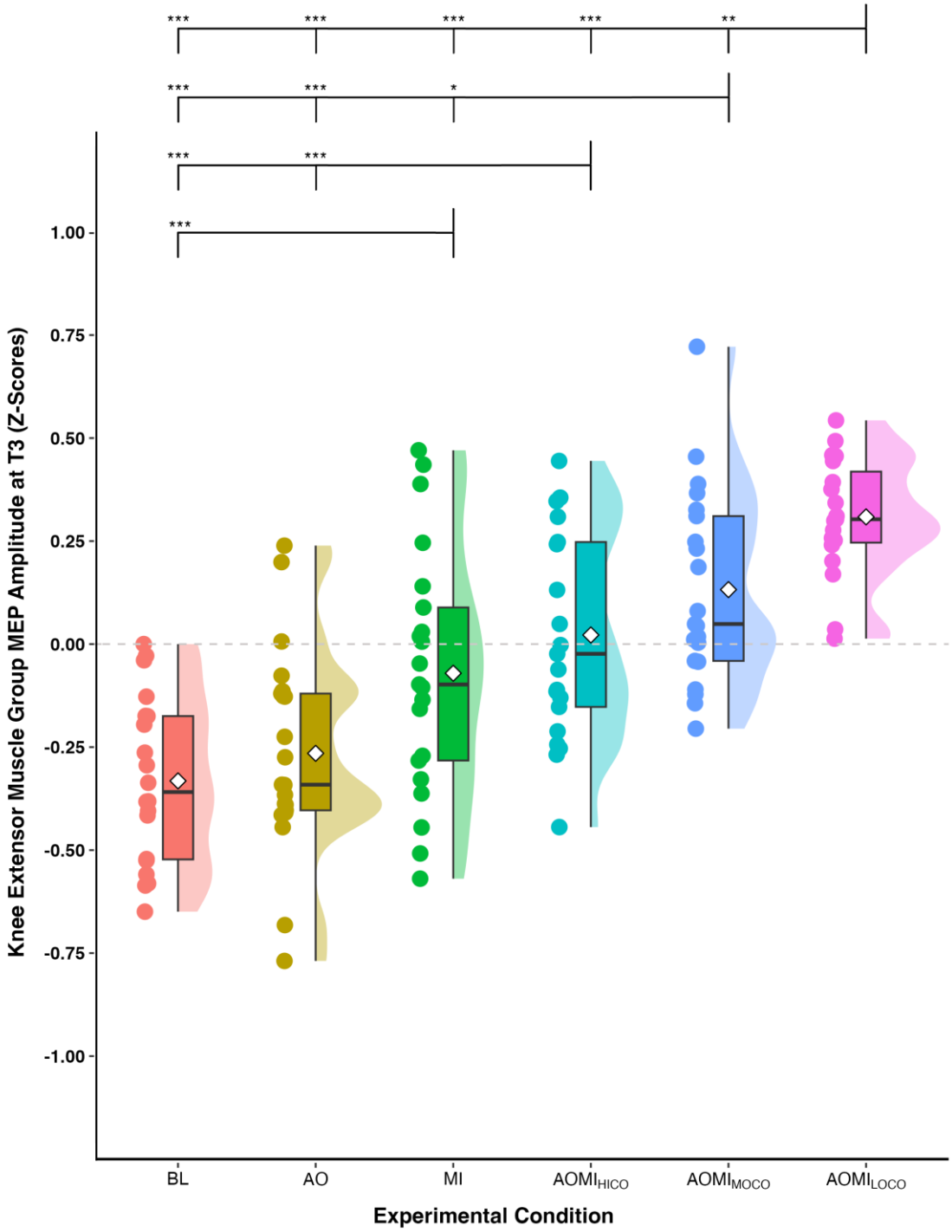

Figure 3. Box and violin plot with raw data points displaying z-score normalized MEP amplitudes from the knee extensor muscle group at the stimulation timepoint corresponding to the *slow-paced* SL-STS (T3) for the three control and three experimental conditions. *Note:* Thick horizontal black lines represent the median average and white diamonds represent the mean average for each box plot. Individual participant data points are represented by circular markers. BL – baseline; AO – action observation; MI – motor imagery; AOMI$_{HICO}$ – highly-coordinated action observation and motor imagery; AOMI$_{MOCO}$ – moderately-coordinated action observation and motor imagery; AOMI$_{LOCO}$ – lowly-coordinated action observation and motor imagery; *$p < .05$, **$p < .01$, ***$p < .001$.

Moderately-Coordinated AOMI ($AOMI_{MOCO}$)

Post-hoc pairwise comparisons at T2 (Figure 4), the TMS stimulation timepoint corresponding to the *medium-paced* SL-STS, showed that *Z*-score MEP amplitudes were significantly larger in the $AOMI_{MOCO}$ condition compared to the BL ($p = .01$) and AO ($p = .02$) conditions, but not the MI condition ($p = .07$). Post-hoc pairwise comparisons at T3 (Figure 3), the TMS stimulation timepoint corresponding to the *slow-paced* SL-STS, showed that *Z*-score MEP amplitudes were significantly larger in the $AOMI_{MOCO}$ condition compared to the BL ($p < .001$), AO ($p < .001$) and MI ($p = .02$) conditions. Post-hoc pairwise comparisons at T1 (Figure 5), the TMS stimulation timepoint corresponding to the *fast-paced* SL-STS, showed that Z-score MEP amplitudes were significantly larger in the $AOMI_{MOCO}$ condition compared to the BL ($p = .04$) and AO ($p = .01$) conditions, but not the MI condition ($p = .56$).

Lowly Coordinated-AOMI ($AOMI_{LOCO}$)

Post-hoc pairwise comparisons at T1 (Figure 5), the TMS stimulation timepoint corresponding to the *fast-paced* SL-STS, showed that *Z*-score MEP amplitudes were significantly larger in the $AOMI_{LOCO}$ condition compared to the BL ($p < .001$), AO ($p < .001$), and MI conditions ($p < .001$). Post-hoc pairwise comparisons at T2 (Figure 4), the TMS stimulation timepoint corresponding to the *medium-paced* SL-STS, showed that *Z*-score MEP amplitudes were significantly larger in the $AOMI_{LOCO}$ condition compared to the BL ($p = .01$), AO ($p = .01$), and MI conditions ($p = .02$). Post-hoc pairwise comparisons at T3 (Figure 3), the TMS stimulation timepoint corresponding to the *slow-paced* SL-STS, showed that *Z*-score MEP amplitudes were significantly larger in the $AOMI_{LOCO}$ condition compared to the BL ($p < .001$), AO ($p < .001$), and MI conditions ($p < .001$).

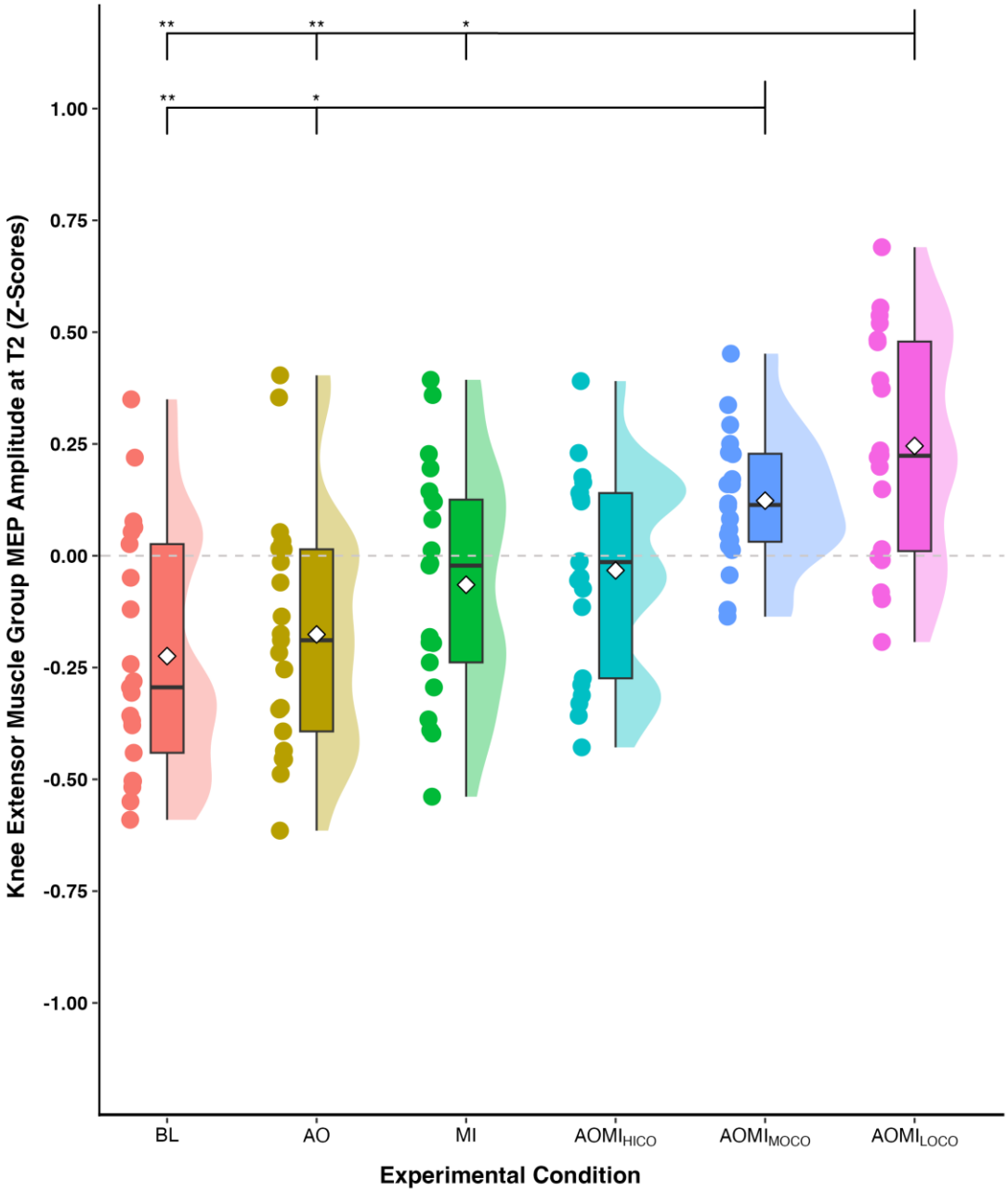

Figure 4. Box and violin plot with raw data points displaying z-score normalized MEP amplitudes from the knee extensor muscle group at the stimulation timepoint corresponding to the *medium-paced* SL-STS (T2) for the three control and three experimental conditions. *Note:* Thick horizontal black lines represent the median average and white diamonds represent the mean average for each box plot. Individual participant data points are represented by circular markers. BL – baseline; AO – action observation; MI – motor imagery; AOMI$_{HICO}$ – highly-coordinated action observation and motor imagery; AOMI$_{MOCO}$ – moderately-coordinated action observation and motor imagery; AOMI$_{LOCO}$ – lowly-coordinated action observation and motor imagery; *$p < .05$, **$p < .01$.

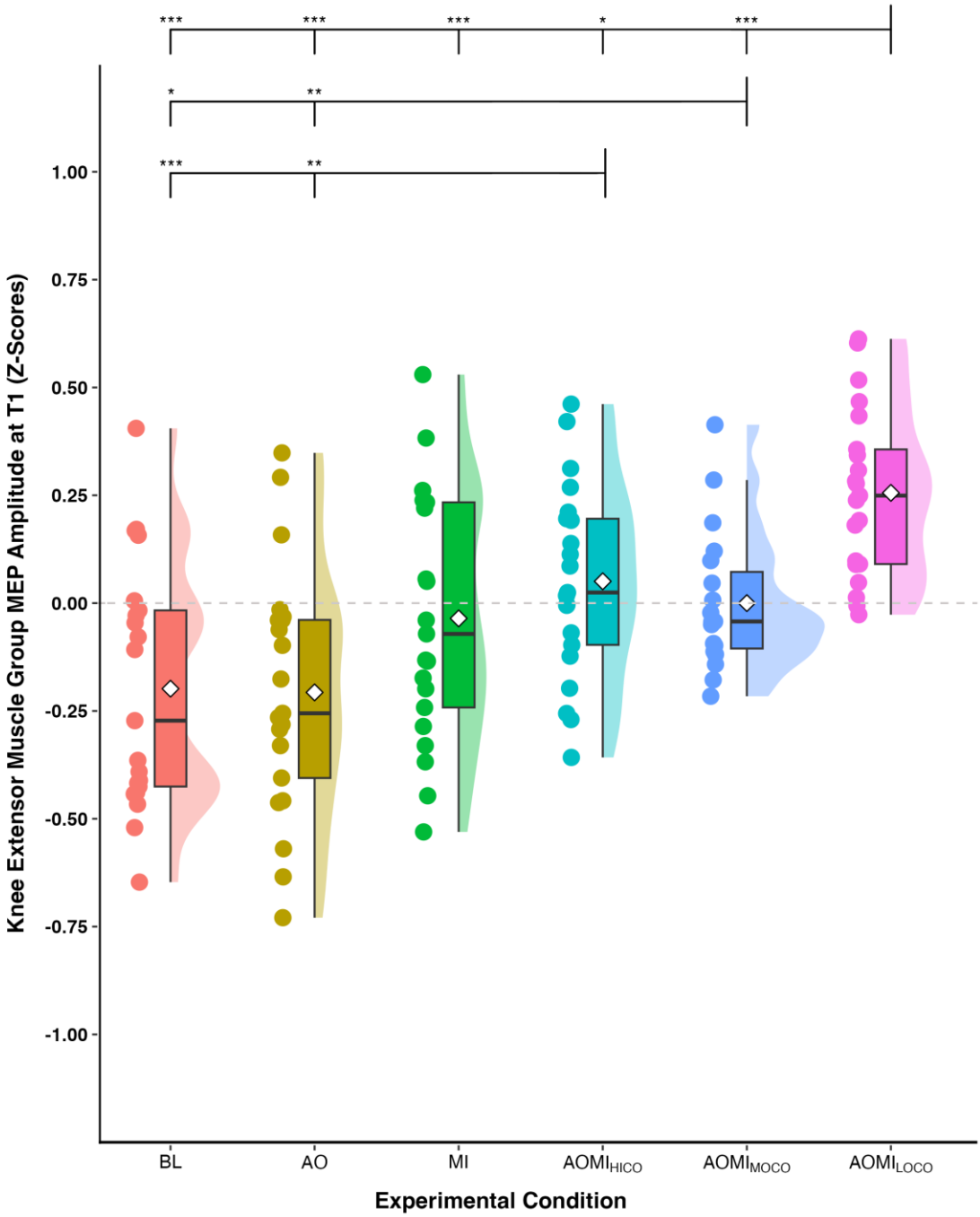

Figure 5. Box and violin plot with raw data points displaying z-score normalized MEP amplitudes from the knee extensor muscle group at the stimulation timepoint corresponding to the *fast-paced* SL-STS (T1) for the three control and three experimental conditions. *Note:* Thick horizontal black lines represent the median average and white diamonds represent the mean average for each box plot. Individual participant data points are represented by circular markers. BL – baseline; AO – action observation; MI – motor imagery; AOMI$_{HICO}$ – highly-coordinated action observation and motor imagery; AOMI$_{MOCO}$ – moderately-coordinated action observation and motor imagery; AOMI$_{LOCO}$ – lowly-coordinated action observation and motor imagery; *$p < .05$, **$p < .01$, ***$p < .001$.

508 **Social Validation Data**

509 ***Questionnaire Responses***

510 A one-way repeated measures ANOVA analysis performed on the perceived MI ability data
511 revealed a significant effect of condition $F_{(3, 60)} = 14.23$, $p < .001$, $\eta_p^2 = .14$. Post-hoc pairwise
512 comparisons showed that perceived MI ability scores were significantly larger in the $AOMI_{HICO}$ condition
513 compared to the MI ($p < .001$), $AOMI_{MOCO}$ ($p < .001$), and $AOMI_{LOCO}$ ($p < .001$) conditions. All participants
514 felt like they were looking at a same-sex model, with male participants recording a mean response of
515 1.67 (±0.50) indicating total agreement that the model they watched is male, and female participants
516 recording a mean response of 1.83 (±0.41) indicating total agreement that the model they watched is
517 female. Despite the acknowledgement that the models were the same-sex as the participants, only six
518 participants (28.57%) felt like they were watching their own performance of the *slow-paced* SL-STS.

519 ***Interview Responses***

520 The interview data provided additional detail about the preferences and strategies adopted by
521 the participants across the experimental conditions. Participants provided mixed responses about
522 perceived MI ability across the conditions where MI was instructed. Sixteen participants (76.19%)
523 suggested MI was easiest in the $AOMI_{HICO}$ condition, with most participants outlining that the synchrony
524 between the observed video and the audio sonification of the SL-STS reduced the difficulty of the
525 cognitive task and facilitated their imagery of the movement (e.g., "It was playing at the correct speed,
526 so I didn't even need to do that [synchronize], so all my attention could be focused on imagining the
527 feeling and sensations" [participant 3]). Conversely, thirteen participants (61.90%) indicated that MI was
528 most difficult in the $AOMI_{MOCO}$ condition and eight participants (38.10%) reported that $AOMI_{LOCO}$ was the
529 most challenging condition in terms of MI ability. Participants that found MI most difficult during
530 $AOMI_{MOCO}$ noted that the close overlap between the speed of the AO and MI processes made it harder
531 to time and maintain the imagined *medium-paced* SL-STS (e.g., "I think the one where I imagined the

middle speed with the slow video [$AOMI_{MOCO}$], that was a bit challenging. Maybe because the speeds were much closer as well, so it's a bit more challenging to imagine, to make sure that I'm not slowing the image to match the video" [participant 12]). In a somewhat contradictory manner, participants that found MI most difficult during $AOMI_{LOCO}$ suggested the scale of the difference between AO and MI processes, and the sheer speed of the imagery, made it hard to accurately generate the imagined *fast-paced* SL-STS (e.g., "I found that one the hardest because it was too distanced between the two [observed and imagined movements] and it was negatively impacting the movements I was imagining due to the mixed signals" [participant 5]).

All participants confirmed that they could successfully engage with MI when instructed to across the experiment. Fourteen participants (66.67%) stated that their MI consisted of only kinesthetic aspects for all conditions (e.g., “there's [imagining] the initial sort of force production bit, which is really tight on the quadriceps, and then once you're sort of almost fully extended, that's when [imagining] the feelings of being balanced comes into it." [participant 3]). However, seven participants (33.33%) indicated that they sometimes generated visual images as well as kinesthetic images of the SL-STS, with this largely taking place in the MI condition due to a lack of visual stimuli, or in the AOMI conditions when attempting to reset their timing or attention to the task. Of these, three participants (14.29%) imagined seeing her/himself performing the SL-STS from a first-person visual perspective whilst maintaining kinesthetic imagery (e.g., "That [third-person] is the perspective I have of that person doing it [in the video], but not of me doing it, because I'm not on the outside of me, so I imagine seeing and feeling it as if I'm practicing" [participant 7]). Four participants (19.05%) imagined seeing her/himself performing the SL-STS from a third-person alongside their kinesthetic imagery (e.g., "There was probably moments where I was imagining things from a sagittal plane as the video was showing, but I think a lot of the time my focus was on imagining the feeling of and the kind of sensations involved” [participant 16]).

556 **Discussion**

557 This study aimed to test the DASH (Eaves, Riach, et al., 2016) and VGH (Meers et al., 2020)
558 propositions for *coordinative* AOMI by comparing CSE responses during highly-, moderately-, and lowly-
559 coordinated AOMI for a SL-STS movement. Task-related MI ability and social validation data were also
560 collected to further explain the cognitive processes underpinning any differences in CSE response during
561 these different types of *coordinative* AOMI. CSE was facilitated for $AOMI_{HICO}$ at T3, indicating a combined
562 effect for the observed and imagined *slow-paced* SL-STS. CSE was facilitated for the $AOMI_{MOCO}$ condition
563 at T3 and T2, indicating an effect for the observed *slow-paced* SL-STS and the imagined *medium-paced*
564 SL-STS, respectively. CSE was facilitated for $AOMI_{LOCO}$ at T3 and T1, indicating an effect for the observed
565 *slow-paced* SL-STS and the imagined *fast-paced* SL-STS. However, CSE was facilitated for $AOMI_{MOCO}$ and
566 $AOMI_{LOCO}$ at all three timepoints, $AOMI_{LOCO}$ reported the greatest CSE facilitation at all three timepoints,
567 and facilitation was inversely related to the level of coordination for AOMI at T3 and T2. These findings
568 suggest the increased speed of MI is driving the facilitation in CSE across the study as a whole. Overall,
569 the findings lend possible support to both the DASH and VGH propositions for *coordinative* AOMI, as
570 discussed below.

571 In this experiment, $AOMI_{HICO}$ involved the simultaneous observation and imagery of a *slow-*
572 *paced* SL-STS movement. Our findings align with both the DASH (Eaves, Riach, et al., 2016) and VGH
573 (Meers et al., 2020) propositions for $AOMI_{HICO}$ as CSE facilitation was increased for this condition at T3,
574 the stimulation timepoint for the observed and imagined *slow-paced* SL-STS, compared with BL and AO,
575 but not MI control conditions. This finding agrees with a body of literature showing CSE facilitation for
576 $AOMI_{HICO}$ relative to control and pure AO conditions (e.g., Bruton et al., 2020; Grilc et al., 2024; Wright et
577 al., 2018). Based on the propositions of the DASH (Eaves, Riach, et al., 2016), the CSE facilitation
578 reported for $AOMI_{HICO}$ is caused by the two motor representations for AO and MI of the *slow-paced* SL-
579 STS merging as one sensorimotor stream, leading to widespread activity in the premotor cortex. This

580 merger is likely to cause increased activity in overlapping brain regions for AO and MI, whilst also
581 increasing activity across a wider neural network that involves brain areas solely recruited during AO and
582 MI for the *slow-paced* SL-STS during $AOMI_{HICO}$ (Hardwick et al., 2018; Filimon et al., 2015). An alternative
583 explanation is provided by the VGH (Meers et al., 2020), which argues that the CSE facilitation during
584 $AOMI_{HICO}$ is indicative of a stronger motor representation for MI of the *slow-paced* SL-STS due to the
585 priming effect of AO for the same *slow-paced* SL-STS. The social validation data lends support to this
586 assertion, as participants reported significantly greater MI ability during the $AOMI_{HICO}$ condition
587 compared to all other conditions where MI was instructed in this experiment. Participants reasoned that
588 MI was easier in this condition due to the synchrony between the video demonstration and sonification
589 of the *slow-paced* SL-STS, indicating that the MI component took priority during $AOMI_{HICO}$. As reported in
590 a recent meta-analysis (Chye et al., 2022), CSE facilitation at T3 was descriptively, but not significantly
591 greater for $AOMI_{HICO}$ compared with MI of the *slow-paced* SL-STS. In combination, our CSE and social
592 validation data support the propositions of the VGH that MI is primed during $AOMI_{HICO}$, but indicate that
593 this effect might be minimal, at least for complex whole-body actions like the *slow-paced* SL-STS used in
594 this study.

595 In the current study, $AOMI_{MOCO}$ involved the observation of a *slow-paced* SL-STS and
596 simultaneous imagination of the feelings and sensations involved with a *medium-paced* SL-STS. Our
597 findings align with the DASH (Eaves, Riach, et al., 2016) proposition for *coordinative* AOMI as CSE was
598 facilitated for the $AOMI_{MOCO}$ condition at T3 compared with all three control conditions indicating an
599 effect for the observed *slow-paced* SL-STS, and at T2 compared with BL and AO control conditions
600 indicating an effect for the imagined *medium-paced* SL-STS. This finding is similar to that reported by
601 Bruton et al. (2020) who showed CSE facilitation for both observed and imagined muscles when
602 controlling for visual attention during *coordinative* AOMI of finger movements, but disagrees with the
603 findings of Meers et al. (2020) and Grilc et al. (2024) that showed CSE facilitation for imagined muscles

604 only during *coordinative* AOMI of finger movements and lower-limb movements, respectively. Based on
605 the propositions of the DASH, the requirement to co-represent two related, but not identical,
606 movements during *coordinative* AOMI involves the maintenance of two parallel sensorimotor
607 representations for the observed *slow-paced* SL-STS and imagined *medium-paced* SL-STS as a set of
608 action affordances. The findings for $AOMI_{MOCO}$ in this study indicate that it is possible to simultaneously
609 co-represent two variations of the same SL-STS movement that differ based on the speed (i.e., *slow*- vs.
610 *medium-paced*) of the simulated movement.

611 The social validation questionnaire and interview data collected in this study indicated that
612 participants found it difficult to both observe the *slow-paced* and imagine the *medium-paced* SL-STS
613 movements during the $AOMI_{MOCO}$ condition because of the close overlap between the speed of the
614 movements. Based on the propositions of the VGH (Meers et al., 2020), the imagined *medium-paced* SL-
615 STS is prioritized during $AOMI_{MOCO}$, meaning the motor representation is only maintained for this action
616 and the observed *slow-paced* SL-STS serves as a visual guide to facilitate MI processes. If this proposition
617 held true, CSE would only be facilitated at T2 during $AOMI_{MOCO}$, as per recent findings (Grilc et al., 2024;
618 Meers et al., 2020). This was not the case, as CSE facilitation was increased at both T3 and T2 for this
619 condition, a finding that could be explained by attentional mechanisms underlying engagement with
620 $AOMI_{MOCO}$. It is possible that participants directed their attention towards either the observed or
621 imagined SL-STS movements when engaging in $AOMI_{MOCO}$ to account for the cognitive demands of the
622 task, and support the generation and maintenance of imagery as the effortful form of movement
623 simulation. Indeed, eye movement (Bruton et al., 2020) and electroencephalographic data (Eaves,
624 Behmer et al., 2016) shows that individuals switch their attention between observed and imagined
625 actions during *coordinative* AOMI. The interview findings reported here are consistent with this
626 interpretation, suggesting participants may direct more attention to either the observed or imagined
627 action on a trial-by-trial basis, resulting in CSE facilitation at T2 and T3 when aggregated across the

628 $AOMI_{MOCO}$ condition in-full. It is noteworthy that CSE facilitation is increased for $AOMI_{MOCO}$ compared
629 with AO at both T2 and T3, and MI at T3, suggesting an additive effect beyond AO or MI processes in
630 isolation. This is indicative of co-representation of the two related, but not identical, movements during
631 $AOMI_{MOCO}$ and disagrees with the proposition that MI drives the CSE facilitation resulting from
632 *coordinative* AOMI (Grilc et al., 2024; Meers et al., 2020).

633 In the $AOMI_{LOCO}$ condition used in this study, participants observed a *slow-paced* SL-STS and
634 simultaneously imagined the feelings and sensations involved with a *fast-paced* SL-STS. Our findings
635 disagree with the propositions of both the DASH (Eaves, Riach, et al., 2016) and VGH (Meers et al., 2020)
636 accounts for *coordinative* AOMI as CSE was facilitated for the $AOMI_{LOCO}$ condition at T3 and T1 compared
637 with all other conditions, indicating an effect for both the observed *slow-paced* and imagined *medium-*
638 *paced* SL-STS during $AOMI_{LOCO}$. This finding contrasts most TMS findings on *coordinative* AOMI, as
639 studies have typically reported increased CSE facilitation for the imagined but not the observed action
640 (Grilc et al., 2024; Meers et al., 2020). Given the low coordination between the movement speeds used
641 for AO and MI components of $AOMI_{LOCO}$, the results also warrant comparison with *conflicting* AOMI. In
642 the only TMS study employing a *conflicting* AOMI condition, Bruton et al. (2020) reported no increase in
643 CSE facilitation in the observed and imagined muscles compared to control conditions (BL, AO). The
644 authors also showed that CSE facilitation was increased in the simultaneously observed and imagined
645 muscle during *congruent* AOMI, and imagined muscle during *coordinative* AOMI, when compared to the
646 *conflicting* AOMI condition. This suggests that the $AOMI_{LOCO}$ condition employed in this study is more
647 representative of *coordinative* than *conflicting* AOMI, but this does not explain the facilitation of CSE for
648 both the observed and imagined SL-STS movements during this condition. It is possible that this reflects
649 the maintenance of two parallel sensorimotor streams for the observed and imagined actions, even
650 when there is a sizable temporal discrepancy between the observed and imagined actions during
651 $AOMI_{LOCO}$, aligning with the sentiments of the DASH (Eaves, Riach et al., 2016).

652 An alternative explanation, consistent with the VGH (Meers et al., 2020), is that MI is driving the
653 increased CSE facilitation reported for $AOMI_{LOCO}$ at all three stimulation timepoints. The level of force or
654 effort of an imagined task is represented in corticomotor activity, with higher force/effort demands
655 leading to increased CSE facilitation during MI (e.g., Helm et al., 2015; Tatemoto et al., 2017; Tremblay
656 et al., 2001). In this study, a positive linear relationship was reported between imagery speed during
657 *coordinative* AOMI and CSE facilitation for T2 and T3, and the condition that required the participants to
658 imagine performing the fastest SL-STS (i.e., $AOMI_{LOCO}$) had the greatest CSE facilitation across all three
659 stimulation timepoints. It was expected that $AOMI_{LOCO}$ would lead to CSE facilitation at T1, as this is the
660 stimulation timepoint aligned to peak EMG activity for a physically executed *fast-paced* SL-STS. CSE
661 facilitation at T2 and T3 was not expected for this experimental condition. Able imagers demonstrate
662 smaller time differences, known as mental chronometry, between physical performance and MI trials of
663 the same task (Guillot & Collet, 2005). This is logical given the shared neural pathways for movement
664 execution and movement simulation (Hardwick et al., 2018), but more difficult movement tasks typically
665 lead to greater temporal discrepancies between imagined and executed movements (Guillot & Collet,
666 2005). The social validation data indicated that participants perceived their imagery ability to be lowest
667 during $AOMI_{LOCO}$, with the conflicting speeds for the observed *slow-paced* and imagined *fast-paced* SL-
668 STS movements disrupting their imagery. Despite the use of audio sonification to guide MI during
669 *coordinative* AOMI in this study (see Castro, Bryjka, et al., 2021; Castro, Osman, et al., 2021) it is possible
670 that participants timing of the imagery was delayed across some trials for the $AOMI_{LOCO}$ condition due to
671 the complexity of the task, possibly explaining the increased CSE facilitation across all three stimulation
672 timepoints for this form of *coordinative* AOMI.

673 The findings reported for different forms of *coordinative* AOMI in this study have important
674 implications for motor (re)learning in sports and rehabilitation settings. $AOMI_{HICO}$ is recommended as the
675 optimal form of motor simulation because it addresses the limitations involved with AO or MI alone, and

676 has additive benefits towards motor skill performance compared to these techniques in isolation (Chye
677 et al., 2022; Wright et al., 2022). These performance benefits are supposedly underpinned by synaptic
678 plasticity processes similar to those observed during physical practice (Holmes & Calmels, 2008). The
679 two other types of *coordinative* AOMI employed in this study ($AOMI_{MOCO}$, $AOMI_{LOCO}$) facilitated CSE at
680 stimulation timepoints aligned with the observed and imagined movements. They may therefore have
681 the capacity to benefit (re)learning of variations of the same action or joint actions (Vogt et al., 2013).
682 These *coordinative* AOMI conditions are a viable complementary training method to physical therapy in
683 rehabilitation settings and could be used to promote the (re)learning of actions that are currently
684 impaired or missing from a person's motor repertoire. For example, a post-stroke patient may benefit
685 from observing videos of themselves accurately performing leg movements such as the SL-STS with their
686 non-affected limb, whilst simultaneously imagining the feelings and sensations associated with
687 performing the same or similar leg movements with their impaired limb (e.g., McCormick et al., 2022). In
688 such cases, $AOMI_{MOCO}$ and $AOMI_{LOCO}$ could support motor (re)learning by promoting Hebbian plasticity in
689 a similar manner to that described above for $AOMI_{HICO}$.
690 All four published studies investigating *coordinative* AOMI have examined the
691 neurophysiological mechanisms underpinning engagement in this form of action simulation using TMS
692 (see Bruton et al., 2020; Grilc et al., 2024; Meers et al., 2020 for other published studies). There is a
693 need to empirically test the effectiveness of $AOMI_{MOCO}$ and $AOMI_{LOCO}$ as movement interventions across
694 populations and contexts in order to substantiate propositions that these types of *coordinative* AOMI
695 may be better than $AOMI_{HICO}$ for (re)learning variations of the same movement or joint actions where
696 interpersonal coordination is required (Eaves et al., 2022). Longitudinal research incorporating both
697 neurophysiological and behavioral measures is required to verify the extent to which repeated
698 engagement in different types of *coordinative* AOMI promotes functional connectivity and plasticity
699 changes within the brain, and the association between these neural adaptations and any motor

700 performance and learning improvements after a *coordinative* AOMI intervention period (Bruton et al.,
701 2020; Chye et al., 2022; Grilc et al., 2024).

702 Single-pulse TMS permits time- and muscle-specific measurement of CSE facilitation, and thus
703 allowed the contributions of each simulation state (i.e., the observed and imagined actions) to be
704 distinguished by examining the effects of different types of *coordinative* AOMI on MEP responses in the
705 KE muscle group at three stimulation timepoints (Naish et al., 2014; Rothwell, 1997). However, this
706 study was limited by only recording MEPs from the agonist muscles (i.e., the KE muscle group) for the
707 SL-STS during the different *coordinative* AOMI conditions. Future studies should record topographically
708 map and record EMG from agonist-antagonist pairs to draw more conclusive evidence regarding CSE
709 facilitation for different types of *coordinative* AOMI. Additionally, the single-pulse TMS technique
710 adopted in this study only provides an indication of activity within the motor and premotor cortices of
711 the brain during *coordinative* AOMI. Activity in other brain regions (e.g., rostral prefrontal cortex; Eaves,
712 Behmer et al., 2016) would not have been represented in the MEP responses recorded in this
713 experiment. There is a need to explore the precise anatomical substrates involved in different types of
714 *coordinative* AOMI using neuroscientific methods with superior spatial resolution, such as functional
715 magnetic resonance imaging (fMRI). FMRI research employing multi-voxel pattern analysis has shown it
716 is possible to distinguish between different actions for MI and execution (Pilgramm et al., 2016; Zabicki
717 et al., 2016). Applying this analysis to fMRI data for different types of *coordinative* AOMI could further
718 advance the understanding of the neural mechanisms underpinning this form of dual-action simulation
719 and provide more conclusive evidence regarding the propositions of the DASH (Eaves, Riach, et al.,
720 2016) and VGH (Meers et al., 2020) accounts for *coordinative* AOMI.

721 In conclusion, the findings of this study lend possible support to both the DASH (Eaves, Riach, et
722 al., 2016) and VGH (Meers et al., 2020) propositions for *coordinative* AOMI. Specifically, in partial
723 support of the DASH, all three *coordinative* AOMI conditions resulted in increased CSE facilitation at the

stimulation timepoint aligned with the observed SL-STS, and at the respective stimulation timepoints aligned with the imagined SL-STS movements. This aligned with propositions of the DASH that sensorimotor representations for the observed and imagined SL-STS movements would merge during $AOMI_{HICO}$ and $AOMI_{MOCO}$ due to the coordination between the simulated SL-STS movements, but this was not expected for $AOMI_{LOCO}$ because of the increased competition between the observed and imagined SL-STS movements. More conclusive support was provided for the VGH account of *coordinative* AOMI as CSE was facilitated across all three stimulation timepoints, and a positive linear relationship was evidenced for imagery speed and MEP amplitude across the *coordinative* AOMI conditions, indicating that imagery is likely driving the CSE facilitation present in the data. However, as different speeds of the SL-STS were both observed and imagined during *coordinative* AOMI in this experiment, it is not possible to distinguish between the contributions of AO and MI on a muscle-specific basis. This study builds on existing neurophysiological support for the use of *coordinative AOMI* as a novel alternative method for (re)learning of movements that extend beyond a learner's repertoire, or for joint actions that require coordination with the movements of others.

References

Alaerts K, Swinnen SP, Wenderoth N. 2010. Observing how others lift light or heavy objects: which visual cues mediate the encoding of muscular force in the primary motor cortex? Neuropsychologia. 48(7):2082–2090. https://doi.org/10.1016/j.neuropsychologia.2010.03.029.

Alaerts K, de Beukelaar TT, Swinnen SP, Wenderoth N. 2012. Observing how others lift light or heavy objects: time-dependent encoding of grip force in the primary motor cortex. Psychol Res. 76(4):503–513. https://doi.org/10.1007/s00426-011-0380-1.

Alcazar J, Aagaard P, Haddock B, Kamper RS, Hansen SK, Prescott E, Alegre LM, Frandsen U, Suetta C. 2020. Age- and sex-specific changes in lower-limb muscle power throughout the lifespan. J Gerontol. 75(7):1369–1378. https://doi.org/10.1093/gerona/glaa013.

Bruton AM, Holmes PS, Eaves DL, Franklin ZC, Wright DJ. 2020. Neurophysiological markers discriminate different forms of motor imagery during action observation. Cortex. 124:119–136. https://doi.org/10.1016/j.cortex.2019.10.016.

Buccino G. 2014. Action observation treatment: a novel tool in neurorehabilitation. Philos Trans R Soc B. 369(1644):20130185. https://doi.org/10.1098/rstb.2013.0185.

Castro F, Bryjka PA, Di Pino G, Vuckovic A, Nowicky A, Bishop D. 2021. Sonification of combined action observation and motor imagery: effects on corticospinal excitability. Brain Cogn. 152:105768. https://doi.org/10.1016/j.bandc.2021.105768.

Castro F, Osman L, Di Pino G, Vuckovic A, Nowicky A, Bishop D. 2021. Does sonification of action simulation training impact corticospinal excitability and audiomotor plasticity? Exp Brain Res. 239(5):1489–1505. https://doi.org/10.1007/s00221-021-06069-w.

Chen R, Gerloff C, Classen J, Wassermann EM, Hallett M, G Cohen L. 1997. Safety of different inter-train intervals for repetitive transcranial magnetic stimulation and recommendations for safe ranges of

771 stimulation parameters. Electroencephalogr Clin Neurophysiol Electromyogr Mot Control.
772 105(6):415–421. https://doi.org/10.1016/s0924-980x(97)00036-2.
773 Chipchase L, Schabrun S, Cohen L, Hodges P, Ridding M, Rothwell J, Taylor J, Ziemann U. 2012. A
774 checklist for assessing the methodological quality of studies using transcranial magnetic stimulation
775 to study the motor system: an international consensus study. Clin Neurophysiol. 123(9):1698–1704.
776 https://doi.org/10.1016/j.clinph.2012.05.003.
777 Chye S, Valappil AC, Wright DJ, Frank C, Shearer DA, Tyler CJ, Diss CE, Mian OS, Tillin NA, Bruton AM.
778 2022. The effects of combined action observation and motor imagery on corticospinal excitability
779 and movement outcomes: two meta-analyses. Neurosci Amp Biobehav Rev. 143:104911.
780 https://doi.org/10.1016/j.neubiorev.2022.104911.
781 Cisek P. 2007. Cortical mechanisms of action selection: the affordance competition hypothesis. Philos
782 Trans R Soc B. [accessed 2024 Dec 4];362(1485):1585–1599.
783 https://doi.org/10.1098/rstb.2007.2054.
784 Clark S, Tremblay F, Ste-Marie D. 2004. Differential modulation of corticospinal excitability during
785 observation, mental imagery and imitation of hand actions. Neuropsychologia. 42(1):105–112.
786 https://doi.org/10.1016/s0028-3932(03)00144-1.
787 Condy EE, Miguel HO, Millerhagen J, Harrison D, Khaksari K, Fox N, Gandjbakhche A. 2021.
788 Characterizing the action-observation network through functional near-infrared spectroscopy: a
789 review. Front Hum Neurosci. 15. https://doi.org/10.3389/fnhum.2021.627983.
790 Cuypers K, Thijs H, Meesen RLJ. 2014. Optimization of the transcranial magnetic stimulation protocol by
791 defining a reliable estimate for corticospinal excitability. PLoS ONE. 9(1):e86380.
792 https://doi.org/10.1371/journal.pone.0086380.
793 Devanne H, Lavoie BA, Capaday C. 1997. Input-output properties and gain changes in the human
794 corticospinal pathway. Exp Brain Res. 114(2):329–338. https://doi.org/10.1007/pl00005641.

Eaves DL, Hodges NJ, Buckingham G, Buccino G, Vogt S. 2022 Dec 27. Enhancing motor imagery practice using synchronous action observation. Psychol Res. https://doi.org/10.1007/s00426-022-01768-7.

Eaves DL, Behmer LP, Vogt S. 2016. EEG and behavioural correlates of different forms of motor imagery during action observation in rhythmical actions. Brain Cogn. 106:90–103. https://doi.org/10.1016/j.bandc.2016.04.013.

Eaves DL, Riach M, Holmes PS, Wright DJ. 2016. Motor imagery during action observation: a brief review of evidence, theory and future research opportunities. Front Neurosci. 10. https://doi.org/10.3389/fnins.2016.00514.

Filimon F, Rieth CA, Sereno MI, Cottrell GW. 2014. Observed, executed, and imagined action representations can be decoded from ventral and dorsal areas. Cereb Cortex. 25(9):3144–3158. https://doi.org/10.1093/cercor/bhu110.

Forster KI, Forster JC. 2003. DMDX: A Windows display program with millisecond accuracy. Behav Res Methods Instrum Amp Comput. 35(1):116–124. https://doi.org/10.3758/bf03195503.

Grilc N, Valappil AC, Tillin NA, Mian OS, Wright DJ, Holmes PS, Castelli F, Bruton AM. 2024. Motor imagery drives the effects of combined action observation and motor imagery on corticospinal excitability for coordinative lower-limb actions. Sci Rep. 14(1). https://doi.org/10.1038/s41598-024-63758-6.

Grosprêtre S, Ruffino C, Lebon F. 2015. Motor imagery and cortico-spinal excitability: a review. Eur J Sport Sci. 16(3):317–324. https://doi.org/10.1080/17461391.2015.1024756.

Guillot A, Collet C. 2005. Duration of mentally simulated movement: a review. J Mot Behav. 37(1):10–20. https://doi.org/10.3200/jmbr.37.1.10-20.

Hardwick RM, Caspers S, Eickhoff SB, Swinnen SP. 2018. Neural correlates of action: comparing meta-analyses of imagery, observation, and execution. Neurosci Amp Biobehav Rev. 94:31–44. https://doi.org/10.1016/j.neubiorev.2018.08.003.

819 Helm F, Marinovic W, Krüger B, Munzert J, Riek S. 2015. Corticospinal excitability during imagined and
820 observed dynamic force production tasks: effortfulness matters. Neuroscience. 290:398–
821 405. https://doi.org/10.1016/j.neuroscience.2015.01.050.
822 Hermens H, Freriks B, Merletti R, Stegeman D, Blok J, Rau G, Disselhorst-Klug C, Hagg G. 1999. European
823 recommendations for surface electromyography. Roessingh Research and Development.
824 Herranz-Gómez A, Gaudiosi C, Angulo-Díaz-Parreño S, Suso-Martí L, La Touche R, Cuenca-Martínez F.
825 2020. Effectiveness of motor imagery and action observation on functional variables: an umbrella
826 and mapping review with meta-meta-analysis. Neurosci Amp Biobehav Rev. 118:828–
827 845. https://doi.org/10.1016/j.neubiorev.2020.09.009.
828 Hess CW, Mills KR, Murray NM. 1987. Responses in small hand muscles from magnetic stimulation of the
829 human brain. J Physiol. 388(1):397–419. https://doi.org/10.1113/jphysiol.1987.sp016621.
830 Holmes P, Calmels C. 2008. A neuroscientific review of imagery and observation use in sport. J Mot
831 Behav. 40(5):433–445. https://doi.org/10.3200/jmbr.40.5.433-445.
832 Jeannerod M. 2001. Neural simulation of action: a unifying mechanism for motor cognition.
833 NeuroImage. 14(1):S103–S109. https://doi.org/10.1006/nimg.2001.0832.
834 Kaneko N, Masugi Y, Yokoyama H, Nakazawa K. 2018. Difference in phase modulation of corticospinal
835 excitability during the observation of the action of walking, with and without motor imagery.
836 NeuroReport. 29(3):169–173. https://doi.org/10.1097/wnr.0000000000000941.
837 Kassambara A. 2023. R package version 0.7.2. Rstatix: pipe-friendly framework for basic statistical tests.
838 https://rpkgs.datanovia.com/rstatix/.
839 Keel JC, Smith MJ, Wassermann EM. 2001. A safety screening questionnaire for transcranial magnetic
840 stimulation. Clin Neurophysiol. 112(4):720. https://doi.org/10.1016/s1388-2457(00)00518-6.

841 Kitamura M, Yamamoto K, Oshima A, Kamibayashi K. 2023. Corticospinal excitability during observation
842 of basketball free-throw movement: effects of video playback speed and stimulus timing. Plos One.
843 18(9):e0292060. https://doi.org/10.1371/journal.pone.0292060.
844 Loporto M, Holmes PS, Wright DJ, McAllister CJ. 2013. Reflecting on mirror mechanisms: motor
845 resonance effects during action observation only present with low-intensity transcranial magnetic
846 stimulation. PLoS ONE. 8(5):e64911. https://doi.org/10.1371/journal.pone.0064911.
847 Loporto M, McAllister CJ, Edwards MG, Wright DJ, Holmes PS. 2012. Prior action execution has no effect
848 on corticospinal facilitation during action observation. Behav Brain Res. 231(1):124–129.
849 https://doi.org/10.1016/j.bbr.2012.03.009.
850 MacIntyre TE, Moran AP, Collet C, Guillot A. 2013. An emerging paradigm: a strength-based approach to
851 exploring mental imagery. Front Hum Neurosci. 7. https://doi.org/10.3389/fnhum.2013.00104.
852 Marusic U, Grosprêtre S, Paravlic A, Kovač S, Pišot R, Taube W. 2018. Motor imagery during action
853 observation of locomotor tasks improves rehabilitation outcome in older adults after total hip
854 arthroplasty. Neural Plast. 2018:1–9. https://doi.org/10.1155/2018/5651391.
855 McCormick SA, Ireland C, Yohannes AM, Holmes PS. 2022. Technology-Dependent rehabilitation
856 involving action observation and movement imagery for adults with stroke: can it work? Feasibility
857 of self-led therapy for upper limb rehabilitation after stroke. Stroke Res Treat. 2022:1–10.
858 https://doi.org/10.1155/2022/8185893.
859 Meers R, Nuttall HE, Vogt S. 2020. Motor imagery alone drives corticospinal excitability during
860 concurrent action observation and motor imagery. Cortex. 126:322–333.
861 https://doi.org/10.1016/j.cortex.2020.01.012.
862 Mizuguchi N, Umehara I, Nakata H, Kanosue K. 2013. Modulation of corticospinal excitability dependent
863 upon imagined force level. Exp Brain Res. 230(2):243–249. https://doi.org/10.1007/s00221-013-
864 3649-3.

865 Moreno-Verdú M, Hamoline G, Van Caenegem EE, Waltzing BM, Forest S, Chembila Valappil A, Khan AH,
866 Chye S, Esselaar M, Campbell MJ, et al. 2023 Nov. Guidelines for reporting action simulation studies
867 (GRASS): proposals to improve reporting of research in motor imagery and action observation.
868 Neuropsychologia. 108733. https://doi.org/10.1016/j.neuropsychologia.2023.108733.
869 Moriuchi T, Iso N, Sagari A, Ogahara K, Kitajima E, Tanaka K, Tabira T, Higashi T. 2014. Excitability of the
870 primary motor cortex increases more strongly with slow- than with normal-speed presentation of
871 actions. PLoS ONE. 9(12):e114355. https://doi.org/10.1371/journal.pone.0114355.
872 Moriuchi T, Matsuda D, Nakamura J, Matsuo T, Nakashima A, Nishi K, Fujiwara K, Iso N, Nakane H,
873 Higashi T. 2017. Primary motor cortex activation during action observation of tasks at different video
874 speeds is dependent on movement task and muscle properties. Front Hum Neurosci. 11.
875 https://doi.org/10.3389/fnhum.2017.00010.
876 Mouthon A, Ruffieux J, Wälchli M, Keller M, Taube W. 2015. Task-dependent changes of corticospinal
877 excitability during observation and motor imagery of balance tasks. Neuroscience. 303:535–543.
878 https://doi.org/10.1016/j.neuroscience.2015.07.031.
879 Mouthon AA, Ruffieux J, Keller M, Taube W. 2016. Age-Related differences in corticospinal excitability
880 during observation and motor imagery of balance tasks. Front Aging Neurosci. 8.
881 https://doi.org/10.3389/fnagi.2016.00317.
882 Naish KR, Houston-Price C, Bremner AJ, Holmes NP. 2014. Effects of action observation on corticospinal
883 excitability: muscle specificity, direction, and timing of the mirror response. Neuropsychologia.
884 64:331–348. https://doi.org/10.1016/j.neuropsychologia.2014.09.034.
885 Nicholson V, Watts N, Chani Y, Keogh JW. 2019. Motor imagery training improves balance and mobility
886 outcomes in older adults: a systematic review. J Physiother. 65(4):200–207.
887 https://doi.org/10.1016/j.jphys.2019.08.007.

888 Pilgramm S, de Haas B, Helm F, Zentgraf K, Stark R, Munzert J, Krüger B. 2015. Motor imagery of hand
889 actions: decoding the content of motor imagery from brain activity in frontal and parietal motor
890 areas. Hum Brain Mapp. 37(1):81–93. https://doi.org/10.1002/hbm.23015.
891 Riach M, Wright DJ, Franklin ZC, Holmes PS. 2018. Screen position preference offers a new direction for
892 action observation research: preliminary findings using TMS. Front Hum Neurosci. 12.
893 https://doi.org/10.3389/fnhum.2018.00026.
894 Roberts R, Callow N, Hardy L, Markland D, Bringer J. 2008. Movement imagery ability: development and
895 assessment of a revised version of the vividness of movement imagery questionnaire. J Sport Exerc
896 Psychol. 30(2):200–221. https://doi.org/10.1123/jsep.30.2.200.
897 Robinovitch SN, Feldman F, Yang Y, Schonnop R, Leung PM, Sarraf T, Loughin M. 2013. Video capture of
898 the circumstances of falls in elderly people residing in long-term care: an observational study.
899 *Lancet*. 381(9860):47–54. https://doi.org/10.1016/S0140-6736(12)61263-X
900 Rossini PM, Burke D, Chen R, Cohen LG, Daskalakis Z, Di Iorio R, Di Lazzaro V, Ferreri F, Fitzgerald PB,
901 George MS, et al. 2015. Non-invasive electrical and magnetic stimulation of the brain, spinal cord,
902 roots and peripheral nerves: basic principles and procedures for routine clinical and research
903 application. an updated report from an I.F.C.N. committee. Clin Neurophysiol. 126(6):1071–1107.
904 https://doi.org/10.1016/j.clinph.2015.02.001.
905 Rothwell JC. 1997. Techniques and mechanisms of action of transcranial stimulation of the human motor
906 cortex. J Neurosci Methods. 74(2):113–122. https://doi.org/10.1016/s0165-0270(97)02242-5.
907 Scott M, Taylor S, Chesterton P, Vogt S, Eaves DL. 2017. Motor imagery during action observation
908 increases eccentric hamstring force: an acute non-physical intervention. Disabil Rehabil.
909 40(12):1443–1451. https://doi.org/10.1080/09638288.2017.1300333.

910 Tapanya W, Chamnongkich S. 2014. Relationship between lower limb muscle strength and single-leg sit-
911 to-stand performance in young adults. *Bull Chiang Mai Assoc Med Sci*. 47(3):133. https://he01.tci-
912 thaijo.org/index.php/bulletinAMS/article/view/59978
913 Tatemoto T, Tsuchiya J, Numata A, Osawa R, Yamaguchi T, Tanabe S, Kondo K, Otaka Y, Sugawara K.
914 2017. Real-time changes in corticospinal excitability related to motor imagery of a force control task.
915 Behav Brain Res. 335:185–190. https://doi.org/10.1016/j.bbr.2017.08.020.
916 Taube W, Lorch M, Zeiter S, Keller M. 2014. Non-physical practice improves task performance in an
917 unstable, perturbed environment: motor imagery and observational balance training. Front Hum
918 Neurosci. 8. https://doi.org/10.3389/fnhum.2014.00972.
919 Tremblay, Louis E Tremblay, Daniel F. 2001. Modulation of corticospinal excitability during imagined
920 knee movements. J Rehabil Med. 33(5):230–234. https://doi.org/10.1080/165019701750419635.
921 Vogt S, Rienzo FD, Collet C, Collins A, Guillot A. 2013. Multiple roles of motor imagery during action
922 observation. Front Hum Neurosci. 7. https://doi.org/10.3389/fnhum.2013.00807.
923 Wickham H (2016). ggplot2: Elegant Graphics for Data Analysis. Springer-Verlag New York. ISBN 978-3-
924 319-24277-4, https://ggplot2.tidyverse.org.
925 Williams J, Pearce AJ, Loporto M, Morris T, Holmes PS. 2012. The relationship between corticospinal
926 excitability during motor imagery and motor imagery ability. Behav Brain Res. 226(2):369–375.
927 https://doi.org/10.1016/j.bbr.2011.09.014.
928 Wright DJ, Frank C, Bruton AM. 2021 Sep 4. Recommendations for combining action observation and
929 motor imagery interventions in sport. J Sport Psychol Action. [accessed 2024 Dec 6]:1–
930 13. https://doi.org/10.1080/21520704.2021.1971810.
931 Wright DJ, Williams J, Holmes PS. 2014. Combined action observation and imagery facilitates
932 corticospinal excitability. Front Hum Neurosci. 8. https://doi.org/10.3389/fnhum.2014.00951.

933 Wright DJ, Wood G, Eaves DL, Bruton AM, Frank C, Franklin ZC. 2018. Corticospinal excitability is
934 facilitated by combined action observation and motor imagery of a basketball free throw. Psychol
935 Sport Exerc. 39:114–121. https://doi.org/10.1016/j.psychsport.2018.08.006.
936 Zabicki A, de Haas B, Zentgraf K, Stark R, Munzert J, Krüger B. 2016 Sep 6. Imagined and executed
937 actions in the human motor system: testing neural similarity between execution and imagery of
938 actions with a multivariate approach. Cereb Cortex. https://doi.org/10.1093/cercor/bhw257.
939